NASA TECHNICAL NOTE

NASA TN D-4927
C. 1

A STUDY OF STIFFNESS MATRICES FOR THE ANALYSIS OF FLAT PLATES

by Dennis A. Kross

George C. Marshall Space Flight Center
Huntsville, Ala.

NATIONAL AERONAUTICS AND SPACE ADMINISTRATION • WASHINGTON, D. C. • DECEMBER 1968

NASA TN D-4927

A STUDY OF STIFFNESS MATRICES FOR THE

ANALYSIS OF FLAT PLATES

By Dennis A. Kross

George C. Marshall Space Flight Center
Huntsville, Ala.

NATIONAL AERONAUTICS AND SPACE ADMINISTRATION

TABLE OF CONTENTS

LIST OF ILLUSTRATIONS

LIST OF TABLES

DEFINITION OF SYMBOLS

Standard indicial and matrix notations are used throughout this paper. Repeated indices, unless enclosed by parenthesis, indicate summation. Upper-case Latin indices generally indicate points in space, whereas lower-case Latin indices indicate elements of an array. Greek indices are, in general, associated with the in-plane coordinate system and range from 1 to 2. The following symbols are used.

a	Determinant of $a_{\alpha\beta}$
$a_{\alpha\beta}$	Coefficients of the first fundamental form of the undeformed surface
$\underset{\sim}{a}$	Tangent base vector in the undeformed middle plane
e	Element identification number
f^N	Bilinear nodal function
g_{ij}	Metric tensor in the undeformed state
h	Thickness of plate
$\underset{\sim b}{k}$	Bending stiffness matrix
$\underset{\sim m}{k}$	Membrane stiffness matrix
$\underset{\sim s}{k}$	Shear stiffness matrix
m	Total number of assembled nodes in system
$m_{N\alpha}$	Local nodal moments
$\underset{\sim}{n}$	Unit vector normal to middle plane
p^α	Surface force components
p_{Ni}	Local nodal loads

DEFINITION OF SYMBOLS (Continued)

q_N	Nodal twist
$\underset{\sim}{U}$	Surface displacement vector
$\underset{\sim}{\bar{U}}$	General displacement vector
w	Transverse displacement
X_α	Surface coordinates
$X_{N\alpha}$	Surface coordinates of node N
Z	Normal to the surface coordinate
$\underset{\sim}{A}_\alpha$	Tangent base vector in deformed system
E	Total number of finite elements
E^{ijkl}	Elastic constants
G_{ij}	Metric tensor in the deformed state
$M_{N\alpha}$	Global nodal moments
P	Point on middle surface of undeformed plate
$P*$	Point on deformed middle surface of plate
$\bar{P}$	General point in undeformed plate
$\bar{P}*$	General point in deformed plate
P	Body force
P_{Ni}	Global nodal forces
U	Total strain energy
U_o	Strain energy density

DEFINITION OF SYMBOLS (Concluded)

$U_{N\alpha}$ Global in-plane displacements

$\underset{\sim}{V}$ General vector field

V_{Ne} Local value of $\underset{\sim}{V}$ at node N of element e

V_N Global value of $\underset{\sim}{V}$ at node N

W_N Global transverse displacements

$\gamma_{\alpha\beta}$ Surface strain components

$\bar{\gamma}_{ij}$ Lagrangian strain tensor

$\underset{\sim}{\delta}$ Local generalized nodal displacement vector

$\epsilon_{\alpha\beta}$ Two-dimensional permutation symbol

ξ_N Mixed derivative of w at node N

θ_α Rotation components

$\chi_{\alpha\beta}$ Surface changes of curvature components

$\underset{\sim}{\Delta}$ Global generalized displacement vector

Θ_α Global rotations

Π Total potential energy

Ω Potential energy of extrinsic forces

Ω_{MNe} Homomorphic mapping constants

ACKNOWLEDGEMENT

A STUDY OF STIFFNESS MATRICES FOR THE ANALYSIS OF FLAT PLATES

SUMMARY

The analysis of thin plates in bending is considered with four different rectangular finite element representations. The first representation approximates the transverse displacement by a sixth-order two-dimensional generalization of a Hermitian interpolation polynomial. This representation requires that the Kirchhoff hypothesis be satisfied throughout the element. Therefore the transverse shear strains vanish, and the element exhibits no shear stiffness. The second representation uses a simple bilinear approximation for the transverse displacements and rotations without the Kirchhoff hypothesis. In the latter case both shear-stiffness and bending-stiffness matrices are obtained. The third approximation uses a discrete Kirchhoff hypothesis which introduces a constraint between the transverse nodal displacements and nodal rotations. This case also contains both bending and shear stiffness. The fourth representation uses only the bending stiffness developed in the previous case. This is a logical approximation since the discrete Kirchhoff hypothesis causes the transverse shears to vanish in the limit. Numerical examples are presented to demonstrate the relative accuracy of the finite elements investigated.

INTRODUCTION

General Comments

Since the thickness of a plate is small in comparison with other dimensions, certain simplifying assumptions can be introduced which reduce plate problems to two-dimensional rather than three-dimensional analysis. The well-known Kirchhoff hypothesis is an example; it assumes that lines normal to a plate's middle surface before deformation remain normal after deformation.

Another less restrictive assumption asserts that displacements vary linearly over the plate thickness. All of these assumptions are kinematic in nature; they impose no restrictions on the order of magnitude of the strains in the plane of the plate or on the order of magnitude of the displacements.

When a thin flexible plate is subjected to transverse loads, it displaces normal to its middle plane and forms a curved surface. If the transverse displacements are small in comparison with the thickness of the plate, the strains in the middle surface are usually small and negligible in comparison with those developed in the extreme fibers. If the plate undergoes large transverse displacements, however, significant strains may be developed in the deformed middle plane. On the other hand, if a flexible plate is subjected to sufficiently large loading in its plane, it will buckle laterally, and bending stresses will be developed. Mathematical descriptions of these phenomena involve highly non-linear partial differential equations in the transverse displacements. Few exact solutions to these equations are available in the literature, and, in the case of plates with irregular shapes and boundary conditions, exact solutions are practically intractable even when classical linear theory is used. Because of this difficulty in obtaining exact solutions, numerical methods are often employed to obtain quantitative solutions to these problems.

Among the numerical methods available, the finite element method is appealing and is the technique investigated in this thesis. In the finite element method, a continuous plate is represented by an assembly of small polyhedral plate elements of finite dimension, each of which is assumed to have finite degrees of freedom. The displacement fields within each element are approximated by polynomial functions of the local coordinate system associated with each finite element. These discrete structural elements are interconnected at a finite number of node points. The problem is then reduced to one of determining a finite number of unknowns.

Scope of Paper

Ironically the finite element formulation of plate problems involves some complications not encountered in finite element analyses of three-dimensional bodies. In the three-dimensional body formulation, only the relative displacement of each node point is of concern, whereas in the thin flat-plate formulation, in addition to the relative displacement of the nodes, the relative rotations and twist come into play. Because of these complications most finite element formulations for the analysis of plates involve high-order polynomial approximations

for the transverse displacement field. These approximations prove unwieldy when extending the formulations to shell analyses and to geometrically nonlinear plate-problems.

Several investigations [1-9] have developed linear finite element stiffness matrices for the analysis of thin plates in bending. Of particular interest among these is the paper by Clough and Tocher [2] which investigates the relative accuracy of seven different types of finite element representations. Melosh's paper [4] was the first to utilize a rectangular-shaped finite element representation for the analysis.

Bogner, Fox, and Schmidt [1] presented interpolation formulas in orthogonal curvilinear coordinates, which they used to approximate the displacement field within a finite element of a flat rectangular plate. These interpolation formulas are polynomials of sixth order in the coordinates. Although this representation is highly complex, it yields a stiffness matrix which exhibits good convergence characteristics. This matrix is examined later in this paper.

Utku [8] and Melosh and Utku [9] have developed a triangular discrete element formulation adaptable to shells. This representation utilized simple linear approximations for the displacement and rotation fields. In order to obtain convergence, however, it was necessary to modify the stiffness matrix acquired in this formulation. Several different schemes were utilized to modify the matrix. This approach was abandoned in the present study in hope of obtaining a more rational approach to the problem.

It appears, therefore, that finite element solutions to plate problems in the past have been extremely involved because of the Kirchhoff hypothesis and convergence criteria involving continuity requirements of the slopes. A more simple finite element representation is needed before the method can be extended to general shell problems and nonlinear plate problems.

This paper, therefore, investigates several finite elements based on relatively simple displacement approximations which satisfy the convergence criteria, but with one exception do not satisfy the Kirchhoff hypothesis throughout the element. The purpose of the study is to develop a simple finite element model which converges well enough. The discrete variables selected in this study are the displacements and rotations of the nodal points. Although this paper considers only the classical small deflection theory of plates, the finite element representations presented are ones which lend themself readily to the shell analysis and to nonlinear plate problems. Numerical examples are presented to demonstrate the relative accuracy of the finite elements investigated.

3

KINEMATIC CONSIDERATIONS

The Discrete Model

In finite element formulations of plate problems, a continuous plate, such as that shown in Figure 1a, is represented by an assembly of a finite number E of small plate elements as indicated in Figure 1b. The geometry of a typical element is defined by the location of a number of nodal points on the element's boundaries, connected by smooth curves called nodal lines. In contrast to classical analyses wherein relationships between mean values of certain variables associated with differential elements are obtained and the dimensions of the elements are shrunk to zero as their number becomes infinite, the dimensions of finite elements remain finite throughout the analysis. Ideally these dimensions are small in comparison with characteristic dimensions of the assembled system so that displacement fields within each element are adequately approximated by appropriate functions (usually polynomials) of the coordinates.

In this study the locations of points in the discrete system are given by the curvilinear surface coordinate $X^{\alpha}(\alpha = 1, 2)$ which are embedded in the middle surface of the plate and a coordinate Z normal to the middle surface. The undeformed shape of the middle surface of each finite element is assumed to be a flat, curvilinear quadrilateral, and for convenience the vertices of these quadrilaterals are selected as the nodal points of the elements (Fig. 1b).

A vector field $\underset{\sim}{V}(X^{\alpha}, Z)$ defined throughout the domain D occupied by the distributed plate, identifies with every point P in D a vector $\underset{\sim}{V}(P)$. In the finite element representation of D, the field $\underset{\sim}{V}$ is depicted by a finite set of quantities which represent the values of $\underset{\sim}{V}$ at each nodal point, the values of $\underset{\sim}{V}$ at other points being given by appropriate interpolation formulas. Thus, if there are m nodal points in the discrete model

FIGURE 1. FINITE ELEMENT REPRESENTATION

4

after all elements have been connected together to form a single assembled system and if $V_{\sim N}$ denotes the value of $V_{\sim}$ at node N, then the set $V_N(N = 1, 2, \ldots m)$ is the global representation of the field $V_{\sim}$. On the other hand, if of the totality of E finite elements element e is isolated and examined independently of the other elements, then the field $V_{\sim}$ is characteristized within e by the set $V_{\sim Me}(M = 1, 2, 3, 4)$, where $V_{\sim Me}$ is the value of $V_{\sim}$ at node M of element e. The sets of quantities $V_{\sim Me}(M = 1, 2, 3, 4; e = 1, 2, 3, \ldots E)$ are referred to as local representations of $V_{\sim}$ corresponding to elements $e = 1, 2, 3, \ldots E$.

This distinction between global values $V_{\sim N}$ and local values $V_{\sim Me}$ of the same field $V_{\sim}$ is introduced for convenience. The general behavior of a typical finite element can be described in terms of local values of various fields, independent of its mode of connection with or the behavior of adjacent elements. The local and global values are then related through transformations of the form

$$V_{\sim Me} = \Omega_{MNe} V_{\sim N} \tag{1}$$

wherein $M = 1, 2, 3, 4; N = 1, 2 \ldots m; e = 1, 2 \ldots E$

$$\Omega_{MNe} = \begin{cases} 1 \text{ if node M of element e is identical to node N of the} \\ \quad \text{assembled system} \\ 0 \text{ if otherwise.} \end{cases} \tag{2}$$

The transformation defined in equation (1) is said to establish the connectivity of the discrete system. Mathematically it establishes the required dependencies between local and global values of the field $V_{\sim}$; physically it connects the elements together at their nodes to form a single unit.

Bilinear Vector Field Approximation

This discussion is limited to a typical element of the system. For convenience the element index e is temporarily dropped.

Assume that the components of a vector field within the region of the rectangular finite element can be approximated by the form

$$V^{\alpha} = B^{\alpha} + C^{\alpha}_{\beta} X^{\beta} + D_{\alpha} X^1 X^2 \qquad (3)$$

where B^{α}, C^{α}_{β}, and D^{α} are the undetermined constants.

Let V^{α}_N and X^{α}_N ($N = 1, 2, 3, 4;\ \alpha = 1, 2$) denote respectively the components of the vector field at node N and the surface coordinates of node N of a typical finite element. To obtain the undetermined constants in terms of nodal quantities, equation (3) is evaluated at each of the four node points of the element being considered. Evaluating equation (3) for the component V^1

$$V^1_N = B^1 + C^1_{\beta} X^{\beta}_N + D^1 Y_N \qquad (4)$$

where

$$Y_N = X^1_{(N)}\ X^2_{(N)}\ (\text{no sum on N}) \ . \qquad (5)$$

In matrix form

$$\underset{\sim}{V}^1_N = \underset{\sim}{C}\ \underset{\sim}{b} \qquad (6)$$

where

$$\underset{\sim}{V}^1_N = \{V^1_1, V^1_2, V^1_3, V^1_4\} \qquad (7a)$$

$$\underset{\sim}{b} = \{B^1, C^1_1, C^1_2, D^1\} \qquad (7b)$$

and

$$\underset{\sim}{C} = \begin{bmatrix} 1 & X^1_1 & X^2_1 & Y_1 \\ 1 & X^1_2 & X^2_2 & Y_2 \\ 1 & X^1_3 & X^2_3 & Y_3 \\ 1 & X^1_4 & X^2_4 & Y_4 \end{bmatrix} \qquad (8)$$

Solving equation (6) for $\underset{\sim}{b}$,

$$\underset{\sim}{b} = \underset{\sim}{C}^{-1} \underset{\sim}{V}_N^1 . \tag{9}$$

Treating the other component of the vector field in a similar fashion, we find that

$$B^\alpha = k^N V_N^\alpha$$

$$C_\beta^\alpha = c_\beta^N V_N^\alpha \tag{10}$$

$$D^\alpha = d^N V_N^\alpha$$

where

$$k^N = \mathscr{E}^{NMRS} X_M^1 X_R^2 Y_S$$

$$c_\beta^N = \epsilon_{\lambda\beta} \mathscr{E}^{NMRS} a_M X_R^\lambda Y_S \tag{11}$$

$$d^N = \mathscr{E}^{NMRS} a_M X_R^2 X_S^1$$

and

$$\mathscr{E}^{NMRS} = \frac{1}{C} \epsilon_{NMRS} . \tag{12}$$

In these equations ϵ_{NMRS} is the four-dimensional permutation symbol, C is the determinant of $\underset{\sim}{C}$, and $a_M = 1 (M = 1, 2, 3, 4)$.

Substituting equation (10) into equation (3) gives

$$V^\alpha = k^N V_N^\alpha + c_\beta^N X^\beta V_N^\alpha + d^N X^1 X^2 V_N^\alpha . \tag{13}$$

Further, let

$$f^N = k^N + c_\beta^N X^\beta + d^N X^1 X^2, \tag{14}$$

then

$$V^{\alpha} = f^N \, V_N^{\alpha} \quad . \tag{15}$$

Equation (15) gives the bilinear approximation for the vector field component V^{α} in terms of the nodal values of this vector field. Note that f^N is independent of the direction of the vector component V^{α}.

Lagrangian Strain Tensor

In order to obtain a finite element representation for a thin plate, it is convenient to review briefly the kinematics of thin shells [10]. In the following, Latin indices range from 1 to 3.

The general definition of the Lagrangian strain tensor $\bar{\gamma}_{ij}$ in the case of a three-dimensional continuum is

$$\bar{\gamma}_{ij} = \frac{1}{2} \, (G_{ij} - g_{ij}) \tag{16}$$

where G_{ij} and g_{ij} are the metric tensors in the deformed and undeformed states respectively. If G_{ij} is expressed in terms of g_{ij} and derivatives of the displacemen field $\bar{U}$ and if linear small deflection theory is used, then equation (16) reduces to the linear strain-displacement relations

$$\bar{\gamma}_{ij} = \frac{1}{2} (\bar{U}_{i;j} + \bar{U}_{j;i}) \tag{17}$$

where $\bar{U}_i$ are the covariant components of the displacement vector and the semicolon denotes covariant differentiation with respect to a curvilinear system of convected coordinates $X^{\alpha} (\alpha = 1, 2)$.

Several simplifications of equations (16) and (17) are possible in the case of finite deformations of continuous flat plates. Consider, for example, the initially flat thin plate shown in Figure 2, the geometry of which is described by the curvilinear surface coordinates X^{α} ($\alpha = 1, 2$) and a coordinate Z normal to the middle surface. The position vector of a general point $\bar{P}$ in the undeformed plate is denoted $\bar{r}$. Tangent base vectors in the undeformed middle plane are denoted $a_{\sim \alpha}$ and $n_{\sim}$ denotes a unit normal to the middle plane.
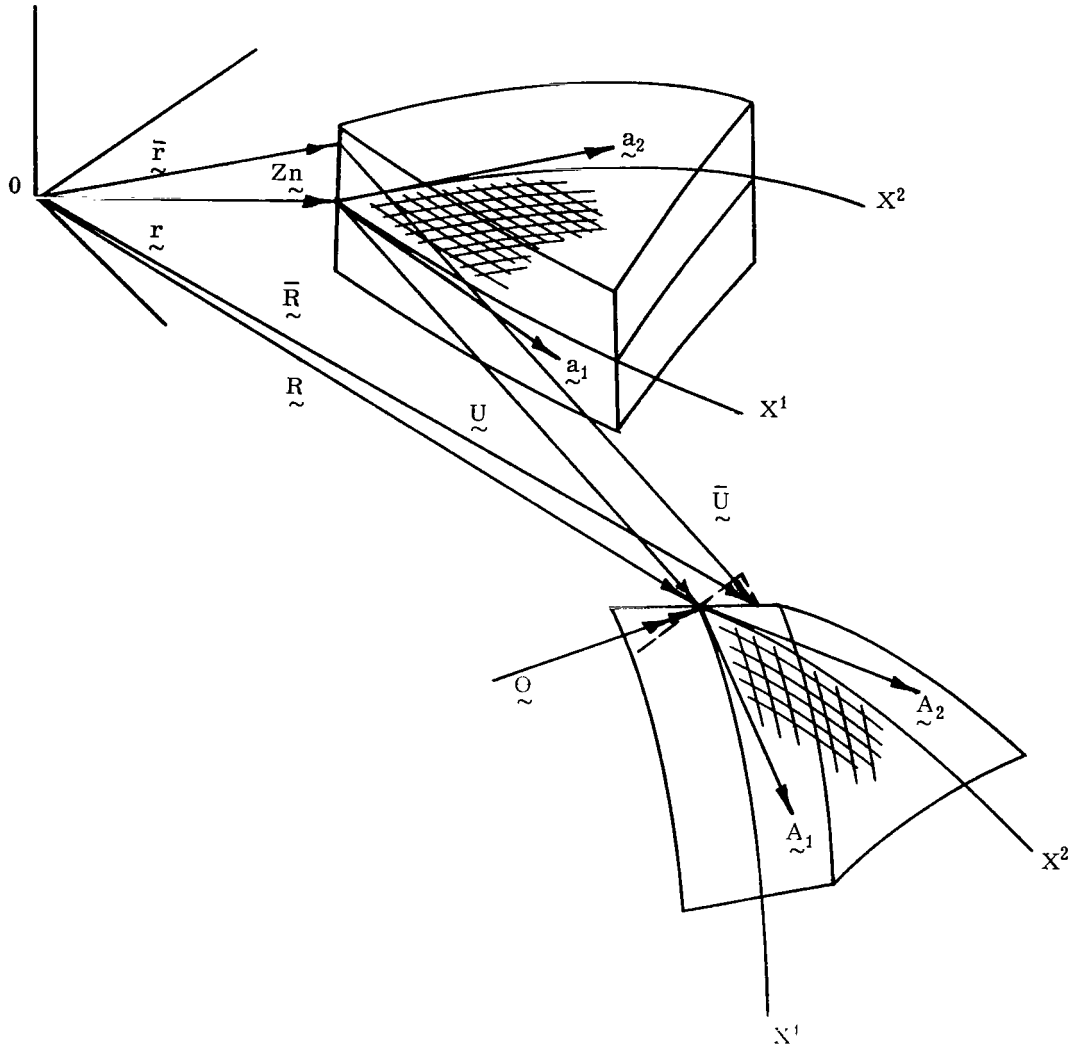
FIGURE 2.   GEOMETRY OF DEFORMATION

If the plate undergoes a general deformation, points $\overline{P}$ and P move with displacement vectors $\overline{U}$ and U to locations $\overline{P}*$ and P*.   In the deformed state point $\overline{P}*$ is located by the position vector $\overline{R}$, and point P* in the deformed middle surface is located by the position vector R, as shown in Figure 2.   The vector initially normal to the middle surface is rotated after deformation.   This rotation vector is denoted Θ.   From Figure 2 it is clearly seen that

$$\overline{U} = U + Z(n \times \Theta) \tag{18}$$

and

9

$$\bar{\underset{\sim}{R}} = \underset{\sim}{R} + Z \underset{\sim}{N} = \underset{\sim}{r} + \underset{\sim}{U} + Z(\underset{\sim}{n} + \underset{\sim}{n} \times \underset{\sim}{\Theta}) \tag{19}$$

where $\underset{\sim}{N}$ denotes a unit vector tangent to the deformed Z coordinate line. The metric tensor in the deformed state is given by

$$G_{\alpha\beta} = \bar{\underset{\sim}{R}},_\alpha \cdot \bar{\underset{\sim}{R}},_\beta . \tag{20}$$

Combining equations (20) and (19) and neglecting nonlinear terms in $\underset{\sim}{U}$ and $\underset{\sim}{\Theta}$ as well as a term involving Z^2, it is found that

$$G_{\alpha\beta} = a_{\alpha\beta} + 2\gamma_{\alpha\beta} + Z\chi_{\alpha\beta} \tag{21}$$

where

$$a_{\alpha\beta} = \underset{\sim}{a}_\alpha \cdot \underset{\sim}{a}_\beta \tag{22}$$

$$2\gamma_{\alpha\beta} = U_{\alpha;\beta} + U_{\beta;\alpha} \tag{23}$$

and

$$\chi_{\alpha\beta} = \sqrt{a} \, (\epsilon_{\lambda\beta} \, \Theta^\lambda_{;\alpha} + \epsilon_{\lambda\alpha} \, \Theta^\lambda_{;\beta}) . \tag{24}$$

In the above equation the determinant of $a_{\alpha\beta}$ is denoted as a. Similarly,

$$G_{\alpha 3} = \bar{\underset{\sim}{R}},_\alpha \cdot \underset{\sim}{N} = w,_\alpha + \sqrt{a} \, \epsilon_{\alpha\lambda} \, \Theta^\lambda . \tag{25}$$

Finally, substituting equations (21) through (25) into equations (16) yields

$$\bar{\gamma}_{\alpha\beta} = \gamma_{\alpha\beta} + Z\chi_{\alpha\beta} \tag{26a}$$

and

$$\bar{\gamma}_{\alpha 3} = w,_\alpha + \sqrt{a} \, \epsilon_{\alpha\lambda} \, \Theta^\lambda . \tag{26b}$$

Note that the transverse extensional strain $\bar{\gamma}_{33}$ was assumed negligible.

10

Kinematics of the Discrete System

To complete the kinematic formulation, it is necessary to obtain the strain displacement relations developed in the preceding section in terms of nodal displacements and rotations. The components of in-plane displacements and rotations may be approximated by a bilinear form. A higher-order form for w, however, will also be investigated. Thus

$$U_\alpha = f^N U_{N\alpha} \tag{27a}$$

$$\Theta^\alpha = f^N \Theta_{N\alpha} \tag{27b}$$

but
$$w = \psi^N w_N \tag{27c}$$

where the special case of $\psi^N = f^N$ is one case to be investigated.

Combining equations (27) with equations (23), (24), and (26),

$$\bar{\gamma}_{\alpha\beta} = \frac{1}{2}\left(f^N_{;\alpha} U_{N\beta} + f^N_{;\beta} U_{N\alpha} \right) + Z\sqrt{a}\left(\epsilon_{\lambda\beta} f^N_{;\alpha} \Theta^\lambda_N + \epsilon_{\lambda\alpha} f^N_{;\beta} \Theta^\lambda_N \right) \tag{28a}$$

and

$$\bar{\gamma}_{\alpha 3} = \psi^N_{,\alpha} w_N + \sqrt{a}\, \epsilon_{\alpha\lambda} f^N \Theta^\lambda_N . \tag{28b}$$

These equations express the strain at any point in a typical plate element in terms of the nodal displacements and nodal rotations. It has been pointed out that the global and local values of a vector field could be related through transformations of the type given by equation (1). Applying these connectivity transformations to the nodal displacements and rotations,

$$U_{M\alpha e} = \Omega_{MNe} U_{N\alpha} \tag{29a}$$

$$w_{Me} = \Omega_{MNe} w_N \tag{29b}$$

$$\Theta^\alpha_{Me} = \Omega_{MNe} \Theta^\alpha_N \tag{29c}$$

where U_N^α, W_N and Θ_N^α are the global values of the in-plane displacements, transverse displacement and rotations at global node N, respectively. The connectivity matrix was defined previously by equation (2).

Combining equations (28) and (29),

$$\bar{\gamma}_{\alpha\beta e} = \frac{1}{2} \left(f_{;\alpha}^N \Omega_{NMe} U_{M\beta} + f_{;\beta}^N \Omega_{NMe} U_{M\alpha} \right)$$

$$+ Z \sqrt{a} \left(\epsilon_{\lambda\beta} f_{;\alpha}^N + \epsilon_{\lambda\alpha} f_{;\beta}^N \right) \Omega_{NMe} \Theta_M^\lambda \qquad (30a)$$

$$\bar{\gamma}_{\alpha 3 e} = \psi_{,\alpha}^N \Omega_{NMe} W_M + \sqrt{a} \, \epsilon_{\alpha\lambda} f^N \Omega_{NMe} \Theta_M^\lambda . \qquad (30b)$$

Equations (30) express the strain in a typical element e of the discrete system in terms of the global nodal displacements and rotations.

STIFFNESS RELATIONS

Local Stiffness Relations

It is possible to develop the stiffness relations for a typical finite element of a thin plate from energy considerations. The total potential energy in an elastic body is given by

$$\Pi = U + \Omega \qquad (31)$$

where $U = \int_V U_o \, dV$ is the total strain energy of the finite element and Ω is the potential energy of the extrinsic forces acting on the body. The potential energy of the extrinsic forces may be written as

$$\Omega = - \int_V p \, w dV - \int_{S_1} p^\alpha \bar{U}_\alpha \, dS_1 \qquad (32)$$

where p is the prescribed body force acting in the Z direction and p^α are the components of the prescribed surface force vectors.

The integration of the surface forces is taken over the area S_1, on which the forces are prescribed. From equation (18) it follows that

$$\bar{U}_\alpha = U_\alpha + Z\sqrt{a}\ \epsilon_{\alpha\beta}\ \Theta^\beta \tag{33}$$

The energy function Ω may now be written in terms of nodal displacements and rotations by combining equations (32), (33), and the approximation equations (27).

$$\Omega = - \int_V p\ \psi^N \sqrt{a}\ dV w_N - \int_{S_1} p^\alpha f^N dS_1\ U_{N\alpha}$$

$$- \int_{S_1} p^\alpha\ Z\sqrt{a}\ \epsilon_{\alpha\beta}\ f_N\ dS_1\ \Theta^\beta_N \tag{34}$$

The nodal quantities have been taken outside the integrals since they are independent of the coordinates X^α, Z. The integral terms in this equation are components of the so-called consistent load vectors and are denoted as

$$p^{N\alpha} = \int_{S_1} p^\alpha f^N dS_1 \tag{35a}$$

$$p^{N3} = \int_V p\ \psi^N \sqrt{a}\ dV \tag{35b}$$

$$m^N_\beta = \int_{S_1} p^\alpha\ Z\sqrt{a}\ \epsilon_{\alpha\beta}\ f^N\ dS_1\ . \tag{35c}$$

where p^{Ni} ($i = 1, 2, 3$; $N = 1, 2, 3, 4$) represents the generalized nodal force acting at node N of a typical element and m^N_α ($\alpha = 1, 2$) represents the generalized nodal moment at node N.

Assuming that the deformation is reversible, either isothermal or adiabatic, an elastic potential function U_o exists which represents the strain energy per unit volume of the undeformed element. The strain energy function can be written in terms of the strains. By means of equations (28), it can also be written in terms of the nodal displacements and rotations. The strain energy density function for an elastic flat plate element is of the form

$$U_o = \frac{1}{2} E^{ijkl} \bar{\gamma}_{ij} \bar{\gamma}_{kl} \tag{36}$$

where E^{ijkl} are elastic constants. The total potential energy is then

$$\Pi = \frac{1}{2} \int_V E^{ijkl} \bar{\gamma}_{ij} \bar{\gamma}_{kl} \, dV - p^{N\alpha} U_{N\alpha}$$

$$- p^{N3} w_N - m^N_\alpha \Theta^\alpha_N \quad . \tag{37}$$

According to the principle of minimum potential energy the strained element reaches an equilibrium state when

$$\frac{\partial \Pi}{\partial U_{N\alpha}} = \frac{\partial \Pi}{\partial w_N} = \frac{\partial \Pi}{\partial \Theta^\alpha_N} = 0 \quad . \tag{38}$$

Thus from equation (37) it follows that

$$p^{N\alpha} = \int_V E^{ijkl} \bar{\gamma}_{ij} \frac{\partial \bar{\gamma}_{kl}}{\partial U_{N\alpha}} \, dV \tag{39a}$$

$$p^{N3} = \int_V E^{ijkl} \bar{\gamma}_{ij} \frac{\partial \bar{\gamma}_{kl}}{\partial w_N} \, dV \tag{39b}$$

$$m^N_\alpha = \int_V E^{ijkl} \bar{\gamma}_{ij} \frac{\partial \bar{\gamma}_{kl}}{\partial \Theta^\alpha_N} \, dV \tag{39c}$$

Since $\bar{\gamma}_{ij}$ are linear functions of the nodal displacements and rotations, the right side of equations (39) are linear functions of these nodal quantities.

Equations (39) may be rewritten in more convenient matrix notation.

$$\underset{\sim}{p} = \underset{\sim}{k} \, \underset{\sim}{\delta} \tag{40}$$

where

14

$$\underset{\sim}{p} = \{p^{11}, p^{21}, \ldots p^{41}, p^{12}, \ldots p^{43}; m_1^1, m_1^2, \ldots m_2^4\} \qquad (41a)$$

and

$$\underset{\sim}{\delta} = \{U_{11}, U_{21}, \ldots U_{41}; U_{12}, \ldots U_{42}; w_1, \ldots w_4; \Theta_1^1, \ldots \Theta_4^1; \Theta_1^2 \ldots \Theta_4^2\} \; .$$

$$(41b)$$

$\underset{\sim}{k}$ is a symmetric matrix which expresses the linear relationship between the generalized nodal forces and displacements for a typical element. It is convenient to express $\underset{\sim}{k}$ by the sum

$$\underset{\sim}{k} = \underset{\sim m}{k} + \underset{\sim b}{k} + \underset{\sim s}{k} \qquad (42)$$

where

$$\underset{m}{k} = \int_V E^{ijkl} \, \bar{\gamma}_{ij} \, \frac{\partial \bar{\gamma}_{kl}}{\partial U_{n\alpha}} \, dV \qquad (43a)$$

$$\underset{\sim b}{k} = \int_V E^{ijkl} \, \bar{\gamma}_{ij} \, \frac{\partial \bar{\gamma}_{kl}}{\partial w_N} \, dV \qquad (43b)$$

$$\underset{\sim s}{k} = \int_V E^{ijkl} \, \bar{\gamma}_{ij} \, \frac{\partial \bar{\gamma}_{kl}}{\partial \Theta_N^\alpha} \, dV \; . \qquad (43c)$$

The $\underset{\sim m}{k}$, $\underset{\sim b}{k}$, and $\underset{\sim s}{k}$ matrices are known as membrane, bending, and shear stiffness matrices, respectively.

Global Stiffness Relations

The stiffness relations derived in the previous section describe the elastic behavior of a single typical rectangular flat plate element relative to a local reference frame. They are independent of the location of the element in the assembled system, the boundary conditions, and the loading conditions. To describe the behavior of a given structure with a specific shape and specific boundary conditions, it is necessary to assemble the elements.

It is convenient to select the local coordinate systems associated with each rectangular element of the assembled system parallel to the global coordinate system. Then it is not necessary to rotate the local nodal vector quantities to the global reference frame.

The transformations of the previous Section, Kinematic Considerations, can be conveniently rewritten in matrix notation by introducing a matrix $\underset{\sim}{\Omega}_e$ such that

$$\underset{\sim}{\delta}_e = \underset{\sim}{\Omega}_e \underset{\sim}{\Delta} \tag{44a}$$

and

$$\underset{\sim}{P} = \underset{\sim}{\Omega}_e \underset{\sim}{p}_e \tag{44b}$$

where

$$\underset{\sim}{\Delta} = \{ U_{11}, \ U_{12}, \ W_1, \ \Theta_1^1, \ \Theta_1^2; \ \dots \ U_{m1}, \ U_{m2}, \ W_m, \ \Theta_m^{\ 1}, \ \Theta_m^{\ 2} \} \tag{45a}$$

and

$$\underset{\sim}{P} = \{ P^{11}, \ P^{12}, \ P^{13}, \ M_1^1, \ M_2^1, \ \dots \ P^{m1}, \ P^{m2}, \ P^{m3}, \ M_1^m, \ M_1^m \} \ . \tag{45b}$$

P^{Ni} and M_α^N are the global values of generalized forces and moments at global node N, respectively. External generalized node forces and generalized node displacements of the assembled system are related by the global stiffness relation

$$\underset{\sim}{P} = \underset{\sim}{K} \underset{\sim}{\Delta} \ . \tag{46}$$

Combining equations (40) , (44) , and (46) ,

$$\underset{\sim}{K} = \sum_{e=1}^{E} \underset{\sim}{\Omega}_e^T \underset{\sim}{k}_e \underset{\sim}{\Omega}_e \ . \tag{47}$$

The matrix $\underset{\sim}{K}$ is known as the total unsupported stiffness matrix for the assembled system. Note that the connectivity relations in equation (47) do not take into account any rotation of coordinate systems since it is assumed that the local and global coordinate systems are parallel.

16

Boundary conditions are next applied to the assembled system by pre-scribing generalized displacements or forces at appropriate nodes. In this way the final *supported stiffness matrix is obtained from the unsupported matrix.* Then equation (46) reduces to a system of independent linear algebraic equations in the unknown nodal displacements and rotations. Once these are solved, the strains are obtained for each element from equations (30). The element stresses σ_e^{ij} may be evaluated by applying the linear stress strain relation

$$\sigma_e^{ij} = E^{ijkl} \bar{\gamma}_{kle} \quad .$$

(48)

This concludes the formulation of the problem. Several special cases are considered in the following section.

PLATE ANALYSES

General Comments

All of the plate stiffness matrices considered in this discussion were developed using the procedure described in the previous Sections specialized to rectangular elements and Cartesian coordinates. Displacement and rotation fields are approximated by relatively simple functions which satisfy the conver-gence criteria but with one exception violate the Kirchhoff hypothesis of normals remaining normal throughout the element. The types of deformation and rotation approximations on which each of the analyses is based will be discussed briefly. The resulting bending, shear, and membrane-stiffness matrices are presented for each case. The coefficients of these stiffness matrices are listed in the Appendix.

Special Cases

As mentioned in the preceding Section, Stiffness Relations, the elemental stiffness matrix may be expressed as a sum of the membrane, bending, and shear matrices.

$$\underset{\sim}{k} = \underset{\sim m}{k} + \underset{\sim b}{k} + \underset{\sim s}{k} \quad .$$

(49)

The membrance stiffness matrix depends on the in-plane displacements but is independent of the transverse displacement w and rotations Θ_α. On the other hand, the in-plane displacements do not influence the bending and shear stiffnesses. The in-plane middle surface displacements are approximated by a bilinear form

$$U_\alpha = f_N\ U_{N\alpha}\ .\tag{50}$$

The strain-displacement relations for a typical element with membrance strains only is of the form

$$2\bar{\gamma}_{\alpha\beta} = U_{\alpha,\beta} + U_{\beta,\alpha}\ .\tag{51}$$

The membrane-stiffness relation is obtained by combining equations (51) and (39a) and is of the form

$$\underset{\sim}{P}_m = \underset{\sim}{k}_m\ \underset{\sim}{U}_m\tag{52}$$

where

$$\underset{\sim}{P}_m = \{p_{11},\ p_{12},\ p_{21},\ p_{22},\ p_{31},\ p_{32},\ p_{41},\ p_{42}\}\tag{53a}$$

and

$$\underset{\sim}{U}_m = \{U_{11},\ U_{12},\ U_{21},\ U_{22},\ U_{31}\ U_{32},\ U_{41},\ U_{42}\}\ .\tag{53b}$$

The coefficients of the membrane stiffness matrix are listed in Table I. All of the cases considered in this report assume the same bilinear form for U_α, and therefore they all have the same membrane stiffness matrix. This matrix has been presented frequently in the literature [1, 7] and is known to yield good results. Therefore, membrane stiffness matrices will not be discussed further.

Case I. The vector field approximation to be utilized in the following cases is of the simple polynomial form. As mentioned earlier, the bilinear approximation is mathematically simpler than the higher order polynomial approximations generally used; however, the relative accuracy obtained from the two different approximations should be compared. Toward this end a higher order polynomial approximation for the transverse displacement field is considered in this case.

18

TABLE I. MEMBRANE STIFFNESS MATRIX

Row	Column							
	1	2	3	4	5	6	7	8
1	$2(b_1 + b_2)$	b_3	$(b_1 - 2b_2)$	b_4	$-(b_1 + b_2)$	$-b_3$	$(-2b_1 + b_2)$	$-b_4$
2		$2(b_5 + b_6)$	$-b_4$	$(2b_5 + b_6)$	$-b_3$	$-(b_5 + b_6)$	b_4	$(b_5 - 2b_6)$
3			$2(b_1 + b_2)$	$-b_3$	$(-2b_1 + b_2)$	b_4	$-(b_1 + b_2)$	b_3
4				$2(b_5 + b_6)$	$-b_4$	$(b_5 - 2b_6)$	b_3	$-(b_5 + b_6)$
5					$2(b_1 + b_2)$	b_3	$(b_1 - 2b_2)$	b_4
6	SYMMETRIC					$2(b_5 + b_6)$	$-b_4$	$(2b_5 + b_6)$
7							$2(b_1 + b_2)$	$-b_3$
8								$2(b_5 + b_6)$

Note: Symbols used in this table are defined in the Appendix.

To simplify the following derivation, fibers initially normal to the middle surface are assumed to remain normal after deformation; that is, the Kirchhoff hypothesis is invoked. Hence the shear strain components are required to vanish. The displacement of any point in the plate is then given by

$$\bar{U}_\alpha = U_\alpha - Zw_{,\alpha} . \qquad (54)$$

The strain displacement relations for this case become

$$2\bar{\gamma}_{\alpha\beta} = U_{\alpha,\beta} + U_{\beta,\alpha} - 2Zw_{,\alpha\beta} \qquad (55)$$

Turning to the representation of w, it is important first to note that it is not sufficient merely to match values of w along the nodal lines to assure monotonic convergence [5]. Because of the Kirchhoff assumptions, plate deformation is dependent on displacements, slopes, twists, curvatures, and so on of the middle surface. Consequently, the displacements of points not on the middle surface represent at best mean values subject to the initial requirement that normals remain normal during deformation. Whereas these assumptions simplify plate analysis, they also impose several restrictions on the form of polynomial approximations of the function w. In fact it can be shown that for monotonic convergence, it is necessary to match not only values of w at boundary points, but also slopes and twists at the corners of the element. With this in mind, the following polynomial approximation for w for a given element is introduced:

$$w = \sum_{r=0}^{3} \sum_{s=0}^{3} A_{rs} (X_1)^r (X_2)^s \; . \tag{56}$$

Here the 16 quantities A_{rs} are undetermined constants.

Let w_N, $\Theta_{N\alpha}$, and ζ_N respectively denote the values of w, the first partial derivatives of $w [\Theta_{N\alpha} = (w_{,\alpha})_N]$, and the mixed derivative of $w [\zeta_N = (w_{,\alpha\beta})_N]$ at node N of a typical finite element. Then

$$w_N = \sum \sum A_{rs} (X_{N1})^r (X_{N2})^s$$

$$\Theta_{N1} = \sum \sum r A_{rs} (X_{N1})^{r-1} (X_{N2})^s \tag{57}$$

$$\Theta_{N2} = \sum \sum s A_{rs} (X_{N1})^r (X_{N2})^{s-1}$$

and

$$\zeta_N = \sum \sum rs A_{rs} (X_{N1})^{r-1} (X_{N2})^{s-1} \; .$$

Equations (57) represent 16 simultaneous equations in the 16 unknowns A_{rs}. Solving these equations, introducing the results into equations (56), and rearranging terms,

$$w = H_N w_N + I_{N\alpha} \Theta_{N\alpha} + J_N \zeta_N \tag{58}$$

where the functions H_N, $I_{N\alpha}$, and J_N are defined in Table II.

It should be noted that this displacement function is a two-dimensional generalization of the Hermite interpolation polynomial [1].

TABLE II. POLYNOMIAL COEFFICIENTS – CASE I

N	H_N	N	I_{N2}
1	$(1 - 3C_1^2 + 2C_1^3)\ (1 - 3C_2^2 + 2C_2^3)$	1	$X_2(1 - 2C_2 + C_2^2)\ (1 - 3C_1^2 + 2C_2^3)$
2	$C_1^2(3 - 2C_1)\ (1 - 3C_2^2 + 2C_2^3)$	2	$X_2C_1^2(1 - C_2)^2\ (3 - 2C_1)$
3	$C_1^2C_2^2(3 - 2C_1)\ (3 - 2C_2)$	3	$X_2C_1^2\ (C_2 - 1)\ (3 - 2C_1)C_2$
4	$C_2^2(3 - 2C_2)\ (1 - 3C_1^2 + 2C_1^3)$	4	$X_2C_2(C_2 - 1)\ (1 - 3C_1^2 + 2C_1^3)$

N	I_{N1}	N	J_N
1	$X_1(1 - 2C_1 + C_1^2)\ (1 - 3C_2^2 + 2C_2^3)$	1	$X_1X_2(1 - 2C_1 + C_1^2)\ (1 - 2C_2 + C_2^2)$
2	$X_1C_1(C_1 - 1)\ (1 - 3C_2^2 + 2C_2^3)$	2	$X_1X_2C_1(C_1 - 1)\ (1 - 2C_2 + C_2^2)$
3	$X_1C_1C_2^2\ (C_1 - 1)\ (3 - 2C_2)$	3	$X_1X_2C_1C_2(1 - C_1)\ (1 - C_2)$
4	$X_1C_2^2(1 - C_1)^2\ (3 - 2C_2)$	4	$X_1X_2C_2(C_2 - 1)\ (1 - 2C_1 + C_1^2)$

Note: Symbols used in this table are defined in the Appendix.

Substituting equation (58) into the strain-displacement relations (55),

$$2\bar{\gamma}_{\alpha\beta} = -2Z(H_{N,\alpha\beta}\ w_N\ I_{N\gamma,\alpha\beta}\ \Theta_{N\gamma} + J_{N,\alpha\beta}\ \zeta_N)\ . \tag{59}$$

The stiffness relation obtained by combining equations (59) and (39b) can be represented by a 16 × 16 bending-stiffness matrix. The bending-stiffness relation is of the form

$$\underset{\sim}{p}_b = \underset{\sim}{k}_b\ \underset{\sim}{U}_b \tag{60}$$

where

$$\underset{\sim}{p}_b = \{p_{13},\ m_{11},\ m_{12},\ q_1;\ p_{23},\ m_{21} \ldots q_4\} \tag{61a}$$

$$\underset{\sim}{U}_b = \{w_1,\ \Theta_{11},\ \Theta_{12},\ \zeta_1;\ w_2,\ \Theta_{21},\ \ldots \zeta_4\} \tag{61b}$$

and q_N represents the twist applied at node N. This finite element formulation was first presented by Bogner, Fox, and Schmidt [1]. The results obtained herein, which were derived independently, are in agreement with those found in Reference 1.

Because of the Kirchhoff hypothesis, the shear stiffness for this case has been assumed zero.

Case II. The second representation studied assumes the transverse displacement w, and the rotations Θ_α may be approximated by bilinear forms

$$w = f_N \, w_N$$

and

$$\Theta_\alpha = f_N \, \Theta_{N\alpha} \quad . \tag{62}$$

Note that this is a special case of equations (27) with $\psi_N = f_N$.

The bending and shear stiffness relations obtained by substituting equations (62) and (28) into equation (39) can be represented as

$$\underset{\sim}{p} = (\underset{\sim}{k}_b + \underset{\sim}{k}_s) \, \underset{\sim}{U} \tag{63}$$

where, for this case,

$$\underset{\sim}{p} = \{p_{13}, \; p_{23}, \; p_{33}, \; p_{43}; \; m_{11}, \; m_{21} \ldots m_{42}\} \tag{64a}$$

and

$$\underset{\sim}{U} = \{w_1, \; w_2, \; w_3, \; w_4; \; \Theta_{11}, \; \Theta_{21}, \; \ldots \; \Theta_{42}\} \quad . \tag{64b}$$

The elements of the bending and shear stiffness matrices obtained for this case are presented in Tables III and IV, respectively.

Case III. It will be shown later that the bilinear approximation considered in Case II results in a representation that converges very slowly. To improve the convergence of the bilinear approximation, a discrete Kirchhoff hypothesis, which imposes constraints on the transverse shears, is introduced in this section. Specifically, it requires that the average transverse shear strain vanish along the edges. This is equivalent to requiring that the transverse shear vanish at the mid-point of each edge since the shear strains are linear along the edges. The geometry of deformation of a typical element edge subjected to this discrete Kirchhoff hypothesis is illustrated in Figure 3.

TABLE III. BENDING STIFFNESS MATRIX – CASE II

Row	Column							
	1	2	3	4	5	6	7	8
1	$2(a_1+a_2)$	$(-2a_1+a_2)$	$-(a_1+a_2)$	(a_1-2a_2)	$-(a_3+a_4)$	(a_3-a_4)	(a_3+a_4)	(a_4-a_3)
2		$2(a_1+a_2)$	(a_1-2a_2)	$-(a_1+a_2)$	(a_4-a_3)	(a_3+a_4)	(a_3-a_4)	$-(a_3+a_4)$
3			$2(a_1+a_2)$	(a_2-2a_1)	(a_3+a_4)	(a_4-a_3)	$-(a_3-a_4)$	(a_3-a_4)
4				$2(a_1+a_2)$	(a_3-a_4)	$-(a_3+a_4)$	(a_4-a_3)	(a_3-a_4)
5					$2(\alpha_1-\alpha_2)$	$(\alpha_1-2\alpha_2)$	$-(\alpha_1+\alpha_2)$	$(\alpha_2-2\alpha_1)$
6	SYMMETRIC					$2(\alpha_1+\alpha_2)$	$(\alpha_2-2\alpha_1)$	$-(\alpha_1+\alpha_2)$
7							$2(\alpha_1+\alpha_2)$	$(\alpha_1-2\alpha_2)$
8								$2(\alpha_1+\alpha_2)$

Note: Symbols used in this table are defined in the Appendix.

TABLE IV. SHEAR STIFFNESS MATRIX – CASE II

Row	Column											
	1	2	3	4	5	6	7	8	9	10	11	12
1	16	8	4	8	0	0	0	0	$12\,d_5$	$6\,d_5$	$-6\,d_5$	$-12\,d_5$
2		16	8	4	0	0	0	0	$6\,d_5$	$12\,d_5$	$-12\,d_5$	$-6\,d_5$
3			16	8	0	0	0	0	$6\,d_5$	$12\,d_5$	$-12\,d_5$	$-6\,d_5$
4				16	0	0	0	0	$12\,d_5$	$6\,d_5$	$-6\,d_5$	$-12\,d_5$
5					16	8	4	8	$-12\,d_4$	$12\,d_4$	$6\,d_4$	$-6\,d_4$
6						16	8	4	$-12\,d_4$	$12\,d_4$	$6\,d_4$	$-6\,d_4$
7							16	8	$-6\,d_4$	$6\,d_4$	$12\,d_4$	$-12\,d_4$
8								16	$-6\,d_4$	$6\,d_4$	$12\,d_4$	$-12\,d_4$
9	SYMMETRIC								$18\,d_1$	$9\,d_2$	$-9\,d_1$	$9\,d_3$
10										$18\,d_1$	$9\,d_3$	$-9\,d_1$
11											$18\,d_1$	$9\,d_2$
12												$18\,d_1$

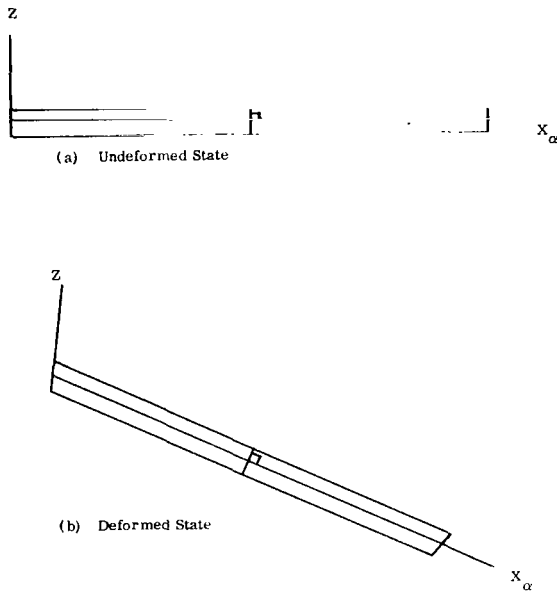Note: Symbols used in this table are defined in the Appendix.

23

z

(a) Undeformed State

z

(b) Deformed State

x_α

FIGURE 3. GEOMETRY OF DEFORMATION OF A TYPICAL ELEMENT EDGE UNDER THE DISCRETE KIRCHHOFF HYPOTHESIS

The discrete Kirchhoff hypothesis introduces a dependence between the rotations $\Theta_{N\alpha}$ and out-of-plane displacements w_N. These relations may be expressed by

$$\underset{\sim}{U} = \underset{\sim}{\psi}\, \underset{\sim}{U}^* \tag{65}$$

where $\underset{\sim}{U}$ is defined by equation (64b) and $\underset{\sim}{U}^*$ is a vector of independent variables which contains eight components. An equivalent load vector $\underset{\sim}{p}^*$ may be obtained by equating the work done in the starred and unstarred system.

$$\underset{\sim}{p}^{*T}\underset{\sim}{U}^* = \underset{\sim}{p}^T\underset{\sim}{U} \ . \tag{66}$$

It follows from equations (64) and (65) that

$$\underset{\sim}{p}^* = \underset{\sim}{\psi}^T \underset{\sim}{p} \ . \tag{67}$$

A stiffness relation is obtained for the starred system by combining equations (63), (65), and (67).

$$\underset{\sim}{p}^* = (\underset{\sim b}{k}^* + \underset{\sim s}{k}^*)\, \underset{\sim}{U}^* \tag{68}$$

where

$$\underset{\sim b}{k}^* = \underset{\sim}{\psi}^T\, \underset{\sim b}{k}\, \underset{\sim}{\psi} \tag{69a}$$

and

$$\underset{\sim s}{k}^* = \underset{\sim}{\psi}^T\, \underset{\sim s}{k}\, \underset{\sim}{\psi} \ . \tag{69b}$$

The elements of the bending and shear-stiffness matrices in the starred system are presented in Tables V and VI, respectively. In these tables the vector of independent variables is defined as

24

$$\underset{\sim}{U}^* = \{ w_1, \ w_2 \ w_3, \ w_4; \ \Theta_{11}, \ \Theta_{21}, \ \Theta_{12}, \ \Theta_{42} \} \ . \tag{70}$$

TABLE V. BENDING STIFFNESS MATRIX – CASES III AND IV

Row	Column							
	1	2	3	4	5	6	7	8
1	$g_1 + 6\lambda$ $+2(g_2 + g_3)$	$-g_1$ $+g_2 - 2g_3$	$g_1 - 6\lambda$ $-g_2 - g_3$	$-g_1$ $-2g_2 + g_3$	bg_4 $+2\mu\alpha_1 a$	bg_5 $+2\mu\alpha_1 a$	$-ag_4$ $-4\mu\alpha_2 b$	$-ag_5$ $-2\mu\alpha_2 b$
2		$g_1 - 6\lambda$ $+2(g_2 + g_3)$	$-g_1$ $+g_3 - 2g_2$	g_1 $-(g_2 + g_3)$	$-bg_4$ $+\mu\alpha_1 a$	$-bg_5$ $+2\mu\alpha_1 a$	$-ag_5$ $+2\mu\alpha_2 b$	$-ag_4$ $+\mu\alpha_2 b$
3			$g_1 + 6\lambda$ $+2(g_2 + g_3)$	$-g_1$ $+(g_2 - 2g_3)$	$-bg_5$ $-\mu\alpha_1 a$	$-bg_4$ $-2\mu\alpha_2 a$	ag_5 $+\mu\alpha_2 b$	ag_4 $+2\mu\alpha_2 b$
4				$g_1 - 6\lambda$ $+2(g_2 + g_3)$	bg_5 $-2\mu\alpha_1 a$	bg_4 $-\mu\alpha_1 a$	ag_4 $-\mu\alpha_2 b$	ag_5 $-2\mu\alpha_2 b$
5					Gb^2 $+4\mu a^2$	$-Gb^2$ $+2\mu a^2$	$-ab\lambda$	$-ab\lambda$
6						$-Gb^2$ $+4\mu a^2$	$-ab\lambda$	$-ab\lambda$
7							Ga^2 $+4\mu b^2$	$-ab\lambda$
8								Ga^2 $+4\mu b^2$

Note: Symbols used in this table are defined in the Appendix.

Case IV.   The main reason for including the transverse shear stiffness in the bilinear approximation is to allow treatment of problems involving forces acting normal to the middle surface.   This results from the bending and membrane stiffness matrices being independent of the out-of-plane displacement w. Since the discrete Kirchhoff hypothesis, however, leads to a dependency between the rotations $\Theta_{N\alpha}$ and displacements w_N, it is no longer necessary to include the shear stiffness in the analysis.   In addition, it is logical to omit the shear stiffness since the discrete Kirchhoff hypothesis causes the transverse shears to vanish in the limit.   Therefore, in this case, the discrete Kirchhoff hypothesis is imposed on the bilinear approximation with the shear stiffness omitted.   The stiffness relation is

$$\underset{\sim}{p}^* = \underset{\sim}{k}_b^* \ \underset{\sim}{U}^* \tag{71}$$

where $\underset{\sim}{k}_b^*$ is the same as in Case III.

TABLE VI.   SHEAR STIFFNESS MATRIX – CASE III

| Row	Column							
	1	2	3	4	5	6	7	8
1	$2\,e_1$	e_2	$-e_1$	e_3	$2\,e_6$	e_6	$-2\,e_5$	$-e_5$
2		$2\,e_1$	e_3	$-e_1$	e_6	$2\,e_6$	$2\,e_5$	e_5
3			$2\,e_1$	e_2	$-e_6$	$-2\,e_6$	e_5	$2\,e_5$
4				$2\,e_1$	$-2\,e_6$	$-e_6$	$-e_5$	$-2\,e_5$
5					$2\,e_4$	e_4	0	0
6	SYMMETRIC					$2\,e_4$	0	0
7							$2\,e_4$	e_4
8								$2\,e_4$

Note: Symbols used in this table are defined in the Appendix.

NUMERICAL EXAMPLES

Square Plate Examples

To test the merits of the stiffness matrices developed in this report, several numerical examples are presented in this Section. Four different plates are considered involving two edge support conditions and two loading conditions. The geometry of the plate and designations are shown in Figure 4.

Because of the symmetry of this problem, only one quadrant of the plate was considered in the analysis. The convergence of each finite element representation was obtained by considering different mesh sizes in the analysis of each case. Figure 5 illustrates the mesh arrangements studied.
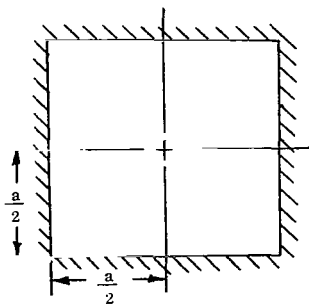
Edge Length = a
Thickness = h

NE · 4

NE = 9

Edges: Simply Supported (SS) or Clamped (C)
Loading: Uniformly Loaded (U) or Concentrated (C)

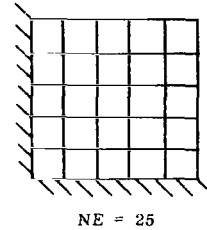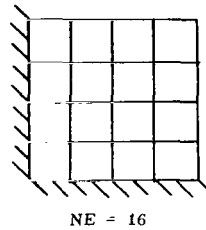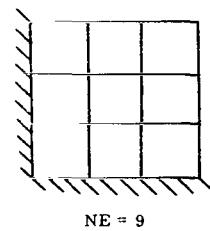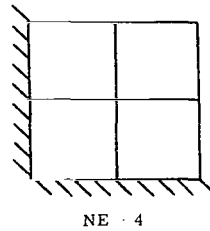| Case	Edges	Load
a	C	U
b	C	C
c	SS	U
d	SS	C

NE = 16

NE = 25

FIGURE 4. GEOMETRY OF PLATE AND CASE DESIGNATIONS

FIGURE 5. TYPICAL FINITE ELEMENT IDEALIZATION

The numerical results obtained in this investigation are presented in Figures 6 through 9. The nondimensional central deflection is presented as a function of the number of elements in a quadrant of the plate. For the case of uniformly loaded plates, the dimensionless central deflection coefficient α is is given by

$$\alpha = \frac{DW_c}{qa^4} \tag{72}$$

where D is the flexural rigidity, W_c is the central deflection, and q is the load intensity.

In the cases of the concentrated load, the deflection coefficient β is defined by

$$\beta = \frac{DW_c}{Pa^2} \tag{73}$$

where P is the concentrated load. The continuum analysis results are from Timoshenko and Woinowsky-Krieger [11]. Since Cases II and III include both bending stiffness, which is proportional to the thickness cubed, and shear stiffness, which is linearly proportional to the thickness, the results for these cases are dependent on the thickness-over-length ratio (h/a). In this analysis the ratio h/a was set equal to 0. 1.

The high-order polynomial approximation of Case I is seen to possess good convergence characteristics, as expected. These results, which were obtained independently, are in agreement with earlier results [1]. It should be emphasized that, because of the high-order polynomial approximation involved in this case, this representation proves cumbersome in the analysis of shells or geometrically nonlinear plate problems. A simple approximation is required to handle more complicated problems.
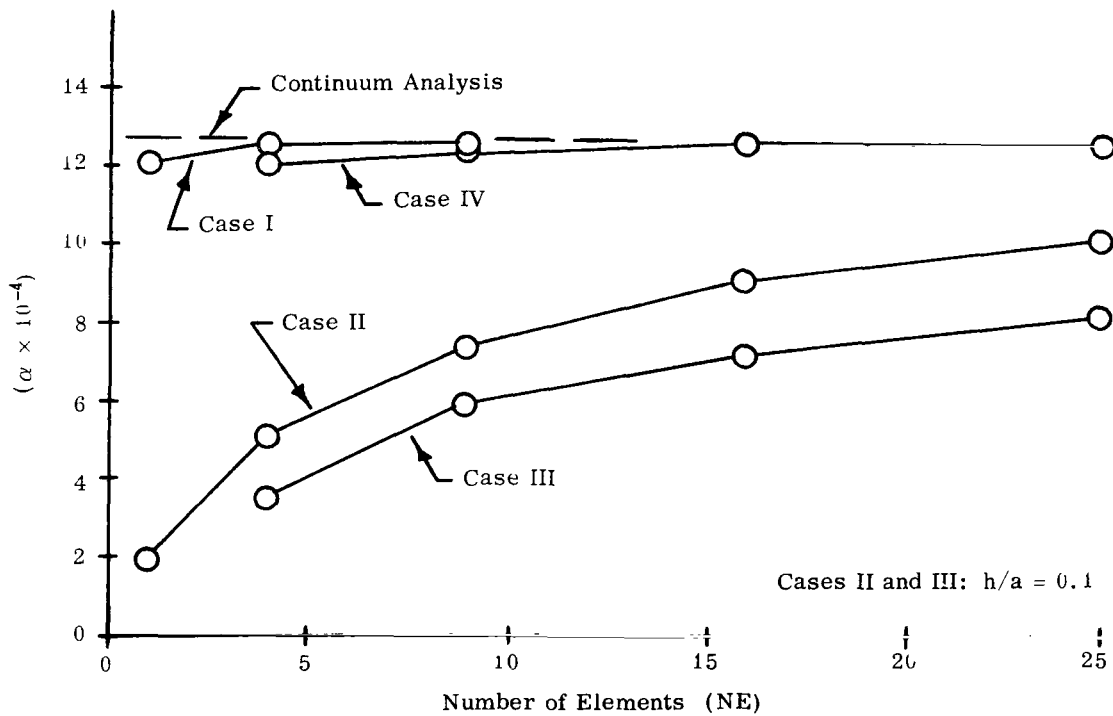

FIGURE 6. CENTRAL DEFLECTION OF A SQUARE
PLATE-CASE a (C - U)

Continuum Analysis

Case I

Case IV

Case II

Case III

Cases II and III: h/a = 0.1

$(\beta \times 10^{-3})$

Number of Elements (NE)
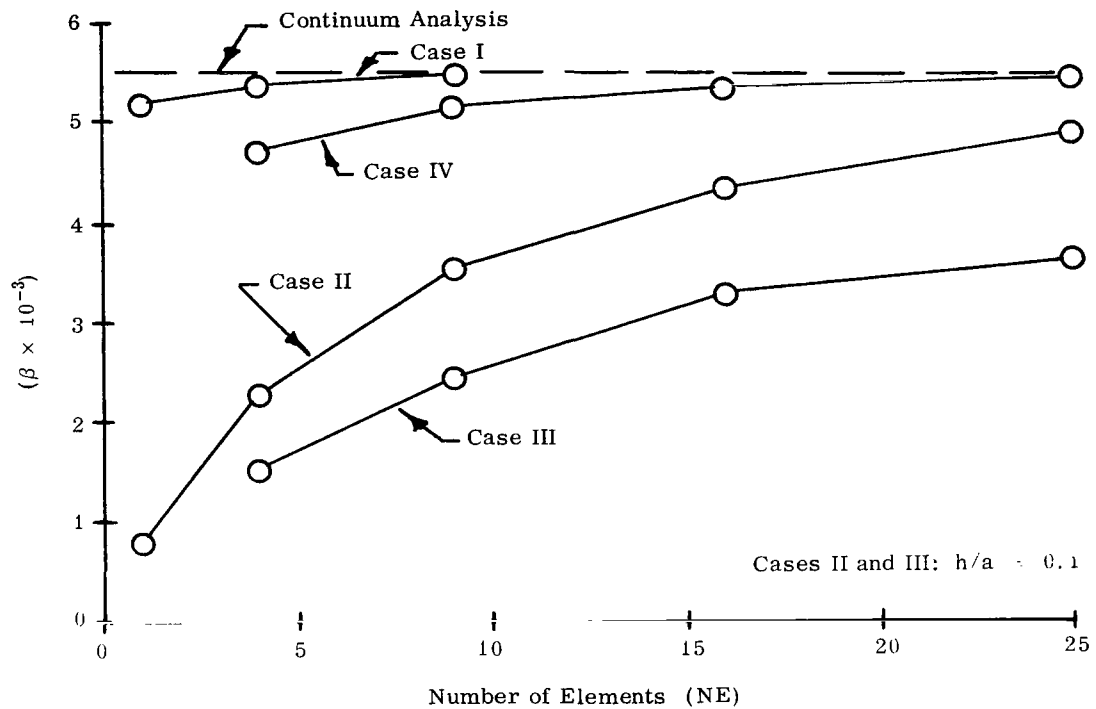
FIGURE 7. CENTRAL DEFLECTION OF A SQUARE PLATE–CASE b (C - C)

Continuum Analysis

Case IV

Case I

Case II

Case III

Cases II and III: h/a = 0.1

$(\alpha \times 10^{-3})$

Number of Elements (NE)

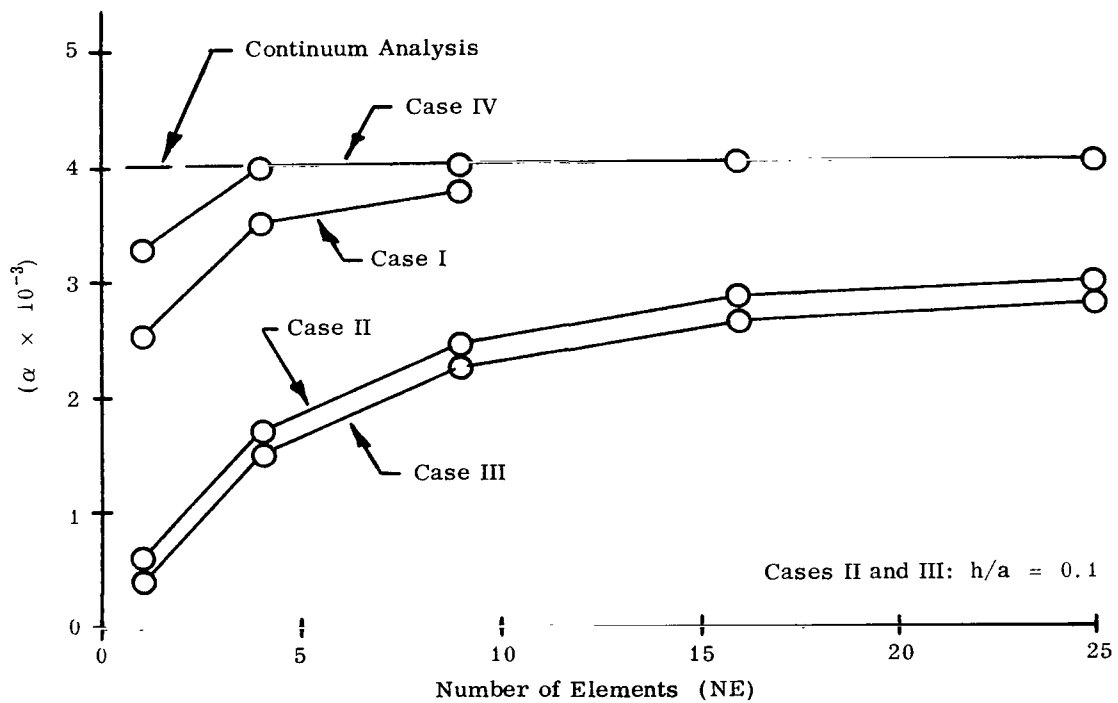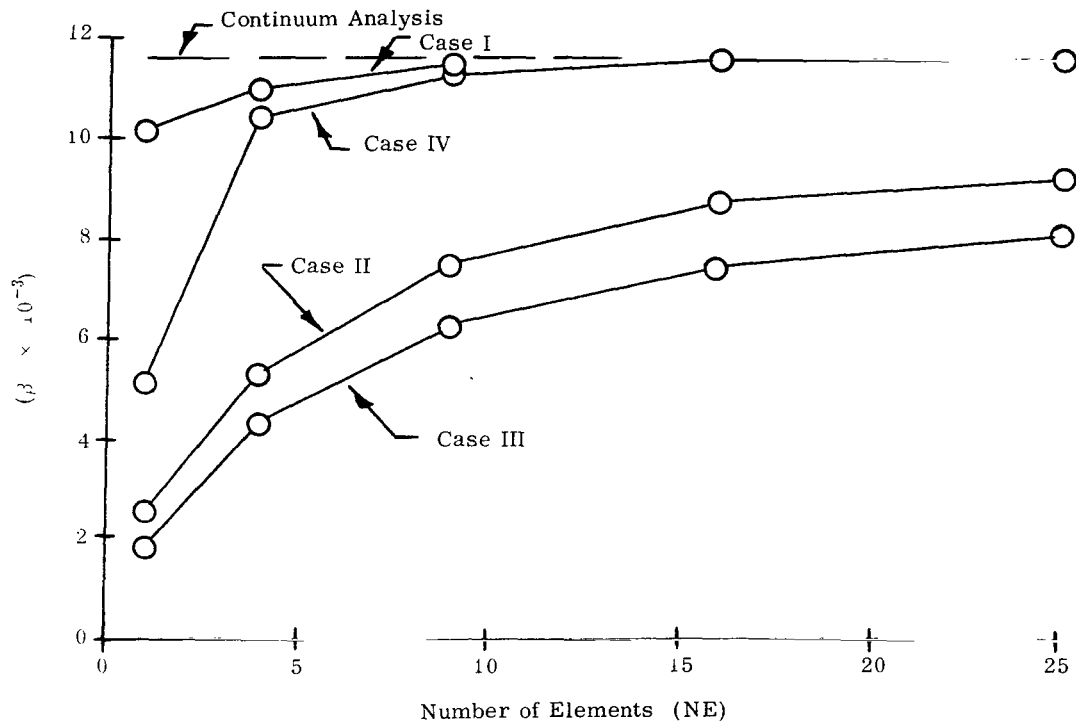FIGURE 8. CENTRAL DEFLECTION OF A SQUARE PLATE–CASE c (SS - U)

29

FIGURE 9.   CENTRAL DEFLECTION OF A SQUARE PLATE-CASE d(SS-C)

It is seen from the graphs that the simple bilinear approximation of Case II yields an element which is too stiff.   This representation forces an unrealistically large portion of the total strain energy to be taken into shear energy. Usually in the analysis of thin plates the shear energy is negligible relative to the energy in bending.   Therefore, the approximations which include the effects of shear, such as Cases II and III, result in an element which is too stiff.   These approximations are more realistic for thicker plates.   Consequently the numerical results of Cases II and III will converge faster for thicker plates.

The Case III representation results in an element which is even stiffer than that of Case II.   In this approximation the shear is constrained to behave in a manner which is realistic for thin plates.   Since, however, the shear energy is still included in the analysis, these constraints tend to make the element unduly stiff.

The Case IV approximation, which simply drops the shear stiffness from the Case III analysis, yields excellent results.   These results are even more surprising because of the fact that this representation has only 16 degrees of freedom as compared with the 24 degrees of freedom of Case I.   In addition, this representation uses a simple bilinear approximation.   This finite element representation appears, therefore, to provide a simple basis for the treatment of plates and shells.

30

Frequently stresses must be computed in addition to the displacement. The stresses may be calculated from the nodal displacements by first applying the strain-displacement relations of equation (30), and then the linear stress-strain relation of equation (48). The finite element method described in this report is based on an assumed displacement pattern. Since the assumed displacement fields are continuous across element boundaries, include possible rigid body motions, and can lead to uniform strain states, the discrete model converges to the true continuum state of deformation as the network is refined. Stresses, however, converge in a mean square sense, but they do not, in general, converge monotonically.

In this study the stresses were calculated at the center of a uniformly loaded simply-supported square plate. The stresses were computed at the four node points nearest the plate's midpoint and then averaged. Figure 10 shows the nondimensional center stress (σ/σ_o) and displacement (w/w_o) as a function of the number of elements, where σ_o and w_o are the results obtained from a continuum analysis [11].
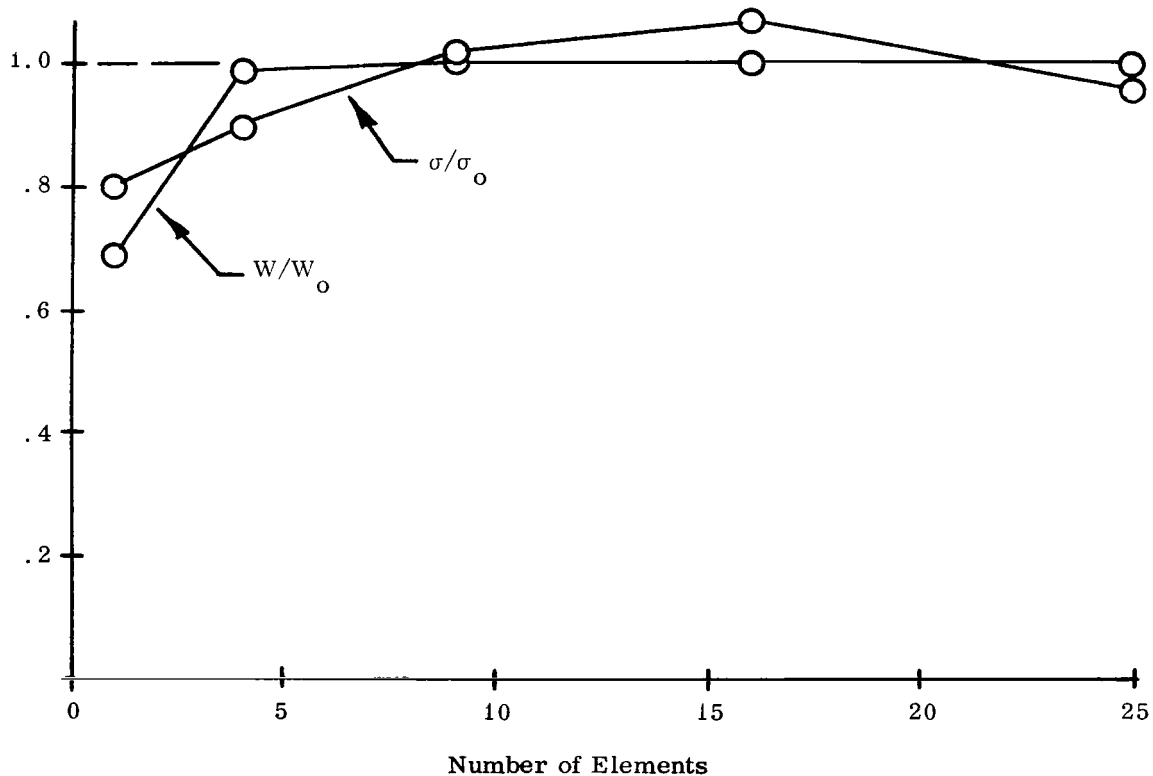

FIGURE 10. CENTRAL STRESS AND DEFLECTION OF A SQUARE SIMPLY-SUPPORTED UNIFORMLY LOADED PLATE

CONCLUSIONS

The high-order polynomial approximation exhibits good convergence characteristics. The simple bilinear approximation with no constraints on the transverse shear strains yields an element that is too stiff. By introducing a discrete Kirchhoff hypothesis into the bilinear approximation and retaining both the bending stiffness and shear stiffness, an element is obtained which is even stiffer. When the shear stiffness is dropped from the discrete Kirchhoff bilinear representation, good convergence is obtained. This last approximation is the simple bilinear form and, in addition, contains only 16 degrees of freedom, whereas the first representation involves a high-order polynomial approximation with 24 degrees of freedom. Therefore, this finite element representation appears to be readily applicable to the analysis of geometrically linear and nonlinear plate and shell problems.

APPENDIX

POLYNOMIAL COEFFICIENTS AND STIFFNESS MATRICES

The polynomial coefficients and stiffness matrices developed in the text are presented in tabular form in this Appendix. Note that the symbols a, b, and h indicate the edge lengths in the X_1 and X_2 directions and the thickness of the plate, respectively. Young's modulus is denoted as E and Poisson's ratio, as ν. A brief explanation of each table follows:

Membrane Stiffness Matrix

The membrane stiffness matrix $\underset{\sim m}{k}$ is found from Table I by first noting that

$$b_1 = \frac{1}{6}\frac{b}{a} \qquad\qquad b_4 = \frac{1-3\nu}{8}$$

$$b_2 = \frac{(1-\nu)}{12}\frac{a}{b} \qquad\qquad b_5 = \frac{1}{6}\frac{a}{b}$$

$$b_3 = \frac{1+\nu}{8} \qquad\qquad b_6 = \frac{(1-\nu)}{12}\frac{b}{a} \qquad\qquad (A-1)$$

and the matrix $\underset{\sim m}{k}^T$ is defined as

$$\underset{\sim m}{k} = K\,\underset{\sim m}{k}^T \qquad\qquad (A-2)$$

where

$$K = \frac{Eh}{(1-\nu^2)} \qquad\qquad (A-3)$$

and $\underset{\sim m}{k}^T$ is the matrix listed in Table I.

Polynomial Coefficients - Case I

Table II lists the coefficients of the Hermitian interpolation polynomial used in the transverse displacements approximation of Case I.   Recalling that

$$w = H_N \, w_N + I_{N\alpha} \, \Theta_{N\alpha} + J_N \, \zeta_N \quad , \qquad (A\text{-}4)$$

the coefficients H_N, $I_{N\alpha}$, and J_N are listed for $N = 1, 2, 3, 4$, $\alpha = 1, 2$.   For convenience the following nondimensional parameters are defined:

$$C_1 = \frac{X_1}{a} \qquad\qquad (A\text{-}5)$$

and

$$C_2 = \frac{X_2}{b} \quad .$$

Bending Stiffness Matrix - Case II

The bending stiffness relation is given by

$$\underset{\sim}{P}_b = \underset{\sim}{k}_b \, \underset{\sim}{U}_b \qquad\qquad (A\text{-}6)$$

where

$$\underset{\sim}{U}_b = \{\Theta_{11}, \ \Theta_{21}, \ \Theta_{31}, \ \Theta_{41}, \ \Theta_{12}, \ \Theta_{22}, \ \Theta_{32}, \ \Theta_{42}\} \qquad (A\text{-}7a)$$

and

$$\underset{\sim}{P}_b = \{m_{11}, \ m_{21}, \ m_{31}, \ m_{41}, \ m_{12}, \ m_{22}, \ m_{32}, \ m_{42}\} \quad . \qquad (A\text{-}7b)$$

The matrix $\underset{\sim}{\underline{k}}_b^T$ listed in Table III is defined by the equation

$$\underset{\sim}{k}_b = \frac{h^3}{48 \, ab} \ \underset{\sim}{k}_b^T \quad . \qquad (A\text{-}8)$$

Table III uses the following nondimensional parameters:

$$a_1 = \frac{Gb^2}{3}$$

$$a_2 = (\lambda + 2G) \frac{a^2}{3}$$

$$a_3 = \lambda \frac{ab}{2}$$

$$a_4 = G \frac{ab}{2} \qquad\qquad (A\text{-}9)$$

$$\alpha_1 = \frac{a}{b}$$

$$\alpha_2 = \frac{b}{a}$$

where

$$G = \frac{E}{2(1+\nu)}$$

and

$$\lambda = \frac{E\nu}{(1-\nu^2)} \qquad\qquad (A\text{-}10)$$

Shear Stiffness Matrix – Case II

The shear stiffness relationship is of the form

$$\underset{\sim}{p}_S = \underset{\sim}{k}_S \underset{\sim}{U}_S \quad , \qquad\qquad (A\text{-}11)$$

where

$$\underset{\sim}{p}_S = \{m_{11}, m_{21}, m_{31}, m_{41}; m_{12}, m_{22}, m_{32}, m_{42}; p_{13}, p_{23}, p_{33}, p_{43}\} \qquad (A\text{-}12)$$

and

$$\underset{\sim S}{U} = \{\Theta_{11}, \Theta_{21}, \Theta_{32}, \Theta_{41}, \Theta_{12}, \Theta_{22}, \Theta_{32}, \Theta_{42}, w_1, w_2, w_3, w_4\} \quad . \quad (A-12b)$$

The matrix $\underset{\sim S}{k}^T$ presented for Case II in Table IV is defined as

$$\underset{\sim S}{k} = \frac{Gh\,ab}{144} \; \underset{\sim S}{k}^T \quad . \tag{A-13}$$

The following parameters are used in the table:

$$d_1 = \frac{8(a^2 + b^2)}{3\,a^2\,b^2}$$

$$d_2 = \frac{8(a^2 - 2b^2)}{3\,a^2\,b^2} \tag{A-14}$$

$$d_3 = \frac{8(b^2 - 2a^2)}{3\,a^2\,b^2}$$

$$d_4 = \frac{2}{a}$$

$$d_5 = \frac{2}{b}$$

Bending Stiffness Matrix – Cases III and IV

The bending stiffness relationship for Cases III and IV is of the form

$$\underset{\sim}{p}^* = \underset{\sim b}{k}^* \; \underset{\sim}{U}^* \tag{A-15}$$

where

$$\underset{\sim}{U}^* = \{W_1, W_2, W_3, W_4, \Theta_{11}, \Theta_{21}, \Theta_{12}, \Theta_{42}\} \quad . \tag{A-16}$$

and

$$\underset{\sim S}{U} = \underset{\sim}{\psi} \; \underset{\sim}{U}^* \tag{A-17}$$

36

where $\underset{\sim}{U}_s$ is defined by equation (A-12b).

It follows that

$$\underset{\sim}{p}^* = \underset{\sim}{\psi}^T \, \underset{\sim}{p}_s \qquad (A\text{-}18)$$

where $\underset{\sim}{p}_s$ is given by equation (A-12a).

The matrix $\underset{\sim}{k}_b^{*\,T}$ presented in Table V is defined by

$$\underset{\sim}{k}_b^* = \frac{h^3}{36\,ab} \; \underset{\sim}{k}_b^{*\,T} \quad . \qquad (A\text{-}19)$$

The following parameters are used in the table:

$$g_1 = 14G$$

$$g_2 = 2\mu\left(\frac{a^2}{b^2}\right)$$

$$g_3 = 2\mu\left(\frac{b^2}{a^2}\right) \qquad (A\text{-}20)$$

$$g_4 = 3\lambda + G$$

$$g_5 = 3\lambda - G$$

and

$$\alpha_1 = \frac{a}{b} \; ; \; \alpha_2 = \frac{b}{a}$$

where

$$\mu = \lambda + 2G \quad .$$

Shear Stiffness Matrix - Case III

The shear stiffness relationship for Case III is of the form

$$\underset{\sim}{p}^* = \underset{\sim s}{k}^* \ \underset{\sim}{U}^* \qquad\qquad (A\text{-}21)$$

where $\underset{\sim}{U}^*$ and $\underset{\sim}{p}^*$ are defined by equations (A-16) and (A-18), respectively. The matrix $\underset{\sim s}{k}^{*\,T}$ presented in Table VI is defined by

$$\underset{\sim s}{k}^* = \frac{Gh}{18\,ab} \ \underset{\sim s}{k}^{*\,T} \quad . \qquad\qquad (A\text{-}22)$$

The following parameters are used in Table VI:

$$e_1 = a^2 + b^2 \qquad\qquad e_4 = a^2 b^2$$

$$e_2 = a^2 - 2b^2 \qquad\qquad e_5 = a b^2 \qquad\qquad (A\text{-}23)$$

$$e_3 = b^2 - 2a^2 \qquad\qquad e_6 = a^2 b$$

REFERENCES

1. Bogner, F. K., Fox, R. L., and Schmidt, L. A. Jr.: The Generation of Interelement, Compatible Stiffness and Mass Matrices by the Use of Interpolation Formulas. Proceedings of Conference on Matrix Methods in Structural Mechanics, Wright-Patterson Air Force Base, Ohio, 1965.

2. Clough, R. W. and Tocher, J. L.: Finite Element Stiffness Matrices for Analysis of Plate Bending. Proceedings of Conference on Matrix Methods in Structural Mechanics, Wright-Patterson Air Force Base, Ohio, 1965.

3. Kapur, K. K. and Hartz, B. J.: Stability of Plates Using the Finite Element Method. Journal of the Engineering Mechanics Division, ASCE, April 1966.

4. Melosh, R. J.: A Stiffness Matrix for the Analysis of Thin Plates in Bending, Journal of the Aeronautical Sciences, vol. 28, No. 34, 1961.

5. Melosh, R. J.: Basis for Derivation of Matrices for the Direct Stiffness Methods. AIAA Journal, vol. 1, No. 7, 1963.

6. Melosh, R. J.: A Flat Triangular Shell Element Stiffness Matrix. Proceedings of Conference on Matrix Methods in Structural Mechanics, Wright-Patterson Air Force Base, Ohio, 1965.

7. Turner, M. J., Cough, R. W., Martin, H. C., and Topp, L. J.: Stiffness and Deflection Analysis of Complex Structures. Journal of the Aeronautical Sciences, vol. 23, No. 9, September 1956.

8. Utku, S.: Stiffness Matrices for Thin Triangular Elements of Nonzero Gaussian Curvature. AIAA 4th Aerospace Sciences Meeting, June 27-29, 1966.

9. Utku, S. and Melosh, R. J.: Behavior of Triangular Shell Element Stiffness Matrices Associated with Polyhedral Deflection Distribution. AIAA 5th Aerospace Sciences Meeting, January 23-26, 1967.

10. Green, A. E. and Zerna, W.: Theoretical Elasticity. Oxford University Press, London, 1954.

11. Timoshenko, S. and Woinowsky-Krieger, S.: Theory of Plates and Shells. McGraw-Hill Book Co., New York, 1959.

POSTMASTER: If Undeliverable (Section 158
Postal Manual) Do Not Return

"*The aeronautical and space activities of the United States shall be conducted so as to contribute ... to the expansion of human knowledge of phenomena in the atmosphere and space. The Administration shall provide for the widest practicable and appropriate dissemination of information concerning its activities and the results thereof.*"

— NATIONAL AERONAUTICS AND SPACE ACT OF 1958

NASA SCIENTIFIC AND TECHNICAL PUBLICATIONS

TECHNICAL REPORTS: Scientific and technical information considered important, complete, and a lasting contribution to existing knowledge.

TECHNICAL NOTES: Information less broad in scope but nevertheless of importance as a contribution to existing knowledge.

TECHNICAL MEMORANDUMS: Information receiving limited distribution because of preliminary data, security classification, or other reasons.

CONTRACTOR REPORTS: Scientific and technical information generated under a NASA contract or grant and considered an important contribution to existing knowledge.

TECHNICAL TRANSLATIONS: Information published in a foreign language considered to merit NASA distribution in English.

SPECIAL PUBLICATIONS: Information derived from or of value to NASA activities. Publications include conference proceedings, monographs, data compilations, handbooks, sourcebooks, and special bibliographies.

TECHNOLOGY UTILIZATION PUBLICATIONS: Information on technology used by NASA that may be of particular interest in commercial and other non-aerospace applications. Publications include Tech Briefs, Technology Utilization Reports and Notes, and Technology Surveys.

Details on the availability of these publications may be obtained from:

SCIENTIFIC AND TECHNICAL INFORMATION DIVISION

NATIONAL AERONAUTICS AND SPACE ADMINISTRATION
Washington, D.C. 20546